Two-photon two-color nuclear magnetic resonance

Cite as: J. Chem. Phys. **121**, 10167 (2004); https://doi.org/10.1063/1.1808697
Submitted: 02 August 2004 . Accepted: 31 August 2004 . Published Online: 11 November 2004

Philip T. Eles, and Carl A. Michal

Two-photon two-color nuclear magnetic resonance

Philip T. Eles and Carl A. Michal[a)]
Department of Physics and Astronomy, University of British Columbia, 6224 Agricultural Road, Vancouver V6T 1Z1, Canada

(Received 2 August 2004; accepted 31 August 2004; publisher error corrected 20 July 2005)

Two-photon excitation has recently been demonstrated to be a practical means of exciting nuclear magnetic resonance (NMR) signals by radio-frequency (rf) irradiation at half the normal resonance frequency. In this work, two-photon excitation is treated with average Hamiltonian theory and shown to be a consequence of higher order terms in the Magnus expansion. It is shown that the excitation condition may be satisfied not only with rf at half resonance, but also with two independent rf fields, where the two frequencies sum to or differ by the resonance frequency. The technique is demonstrated by observation of proton NMR signals at 400 MHz while simultaneously exciting at 30 and 370 MHz. Advantages of this so-called two-color excitation, such as a dramatic increase in nutation rate over half-frequency excitation, along with a variety potential applications are discussed. © *2004 American Institute of Physics.* [DOI: 10.1063/1.1808697]

I. INTRODUCTION

Pulsed NMR has traditionally been performed in two distinct stages:[1] first, nuclear spins are excited by some sequence of radio-frequency (rf) pulses and second, NMR signals are detected as a free induction decay. With the introduction of stroboscopic detection techniques such as CPMG (Ref. 2) and WaHuHa,[3] the two stages may be interleaved but still require the receiver to be turned off during excitation. In practice, probe ringdown and transients from receiver gates impose a receiver dead time[4] that can, in unfavorable cases, last longer than the free induction signal, but more commonly results in distortions to the desired spectra. Recently, it was demonstrated that receiver dead time can be entirely eliminated by exciting nuclear spins with an rf field at half the transition frequency, allowing NMR signals to be acquired *during* excitation.[5] This excitation was denoted ''two photon'' in analogy to the simultaneous absorption of two optical photons.

While nonlinear processes form the basis for a wide variety of important optical techniques and devices, similar effects in NMR, for example, two-photon excitation and the Bloch-Siegert[6] shift, are either little known or viewed as artifacts, and consequently form the basis for few if any common experimental techniques. Even so, multiphoton excitation of magnetic resonance transitions has been known for many years,[7,8] and encompasses a rich variety of processes. These processes may be divided into two broad types, the first involving the absorption of two or more near resonance photons to directly excite transitions between nuclear spin levels with spin quantum number difference $\Delta m \neq \pm 1$, as observed in early cw NMR experiments,[9] while the second type involves the excitation of transitions between levels having $\Delta m = \pm 1$ by a multiphoton process. Of this second type, cases with multiple rf fields near the ordinary resonance frequency have been considered, both in cw (Ref. 10) and in pulsed NMR,[11] while excitation at a submultiple of the resonance frequency has been discussed by Abragam[12] and Shirley.[13]

We distinguish multiphoton excitation from the much more commonly used suite of techniques comprising multiple-quantum NMR,[14] where single-photon processes are used to indirectly excite and detect coherences between nuclear spin levels with $|\Delta m| > 1$.

Our laboratory has recently demonstrated two-photon excitation of NMR (Ref. 5) and NQR (Ref. 15) transitions and shown that such two-photon excitation may be effectively combined[5] with noise spectroscopy (stochastic excitation).[16,17] A principal drawback of two-photon excitation is the relatively low nutation rates produced, requiring either very large applied rf fields or long pulses to produce appreciable tip angles.

In this work, we consider two-photon excitation theoretically using average Hamiltonian theory (AHT) (Ref. 18) and generalize to include excitation with two rf fields at different frequencies. We identify two-photon excitation with the first-order term in the Magnus expansion, and, in solving the case for a single spin, show that the excitation occurs if the frequencies of the two applied rf fields sum to or differ by the transition frequency. Significantly, the rate of nutation increases as the two frequencies deviate from half resonance. We demonstrate this so-called two-color excitation on ^{1}H nuclear spins in water excited at 30 and 370 MHz with detection at 400 MHz, and close with a discussion of some practical considerations for two-color excitation along with potential opportunities for nonlinear phenomena in NMR.

II. THEORY

A. General approach to two-photon excitation from first-order average Hamiltonian theory

The Hamiltonian of a nuclear spin under rf irradiation can be written as

a)Author to whom correspondence should be addressed; Fax: (604) 822-5324. Electronic mail: michal@physics.ubc.ca

$$\hat{\mathcal{H}}(t)=\hat{\mathcal{H}}_{\text{static}}+\gamma\vec{B}_1\cdot\vec{I}\cos\omega_{\text{rf}}t, \tag{1}$$

where $\hat{\mathcal{H}}_{\text{static}}$ is due to some static interaction such as the Zeeman interaction, γ is the gyromagnetic ratio of the nucleus of interest, $\vec{B}_1$ specifies the amplitude and direction of the applied rf field, ω_{rf} is the angular frequency of the rf, and $\vec{I}$ is the spin's angular momentum operator.

Diagonalizing the static Hamiltonian with a change of basis represented by the matrix A (yielding the eigenvalues ω^i) and transforming into an interaction representation via $\hat{U}=e^{-i(A^{-1}\hat{\mathcal{H}}_{\text{static}}A)t}$ removes the effect of the static interaction leaving

$$\hat{\mathcal{H}}_{\text{eff}}(t)=\hat{U}^{\dagger}A^{-1}(\gamma\vec{B}_1\cdot\vec{I})A\hat{U}\cos\omega_{\text{rf}}t. \tag{2}$$

The element in the ith row and jth column of $\hat{\mathcal{H}}_{\text{eff}}$ has the following time dependence:

$$[\hat{\mathcal{H}}_{\text{eff}}(t)]_{ij}=[\hat{\mathcal{H}}_{\text{eff}}(0)]_{ij}e^{i(\omega^i-\omega^j)t}\cos\omega_{\text{rf}}t. \tag{3}$$

For $i=j$, the only time dependence is in the cosine, while for $i\neq j$, there is a time dependence corresponding to the transition frequency between the ith and jth eigenstates. Thus the effective Hamiltonian can be decomposed into terms according to their time dependences:

$$\hat{\mathcal{H}}_{\text{eff}}(t)=\left[\hat{\mathcal{H}}^0+\sum_n\hat{\mathcal{H}}^n e^{i\omega_n t}\right]\cos\omega_{\text{rf}}t, \tag{4}$$

where we sum over the transitions, labeled by the index n, having frequencies ω_n.

From AHT, the leading order effect of a time-dependent Hamiltonian is given by the first nonzero term in the Magnus expansion, where the zeroth- and first-order terms are given by[19]

$$\overline{\mathcal{H}^{(0)}_{\text{eff}}}=\frac{1}{t}\int_0^t dt'\hat{\mathcal{H}}_{\text{eff}}(t') \tag{5}$$

$$\overline{\mathcal{H}^{(1)}_{\text{eff}}}=\frac{-i}{2t}\int_0^t dt'\int_0^{t'}dt''[\hat{\mathcal{H}}_{\text{eff}}(t'),\hat{\mathcal{H}}_{\text{eff}}(t'')]. \tag{6}$$

Although AHT is more commonly applied to systems evolving under cyclic Hamiltonians,[18] it is valid here as long as all time-dependent terms in the integrand vary rapidly compared to the time scale of spin evolution in the interaction frame. The integrals of Eqs. (5) and (6) then display brief transients, but rapidly converge to steady-state values. For convenience we evaluate the integrals in the limit $t\to\infty$.

From the orthogonality of trigonometric functions under integration over time, it is clear from Eqs. (4) and (5) that the zeroth-order term will vanish unless the rf is applied on-resonance for one of the transition frequencies ($\omega_{\text{rf1}}=\omega_n$), in which case it becomes $\overline{\mathcal{H}^{(0)}_{\text{eff}}}=\hat{\mathcal{H}}^n/2$.

For two-photon excitation of the nth transition at half the transition frequency, $\omega_{\text{rf}}=\omega_n/2$, the zeroth-order Hamiltonian will always vanish. However, there will be a first-order contribution that survives due to cross terms between $\hat{\mathcal{H}}^0$ and $\hat{\mathcal{H}}^n$ (i.e., integrands of the form $e^{i\omega_n t'}\cos\omega_{\text{rf1}}t'\cos\omega_{\text{rf1}}t''$). It is exactly these cross terms that result in two-photon excitation for $\omega_{\text{rf}}=\omega_n/2$.

TABLE I. Integrals for Eq. 6 for noninteger δ/ω_0. Each entry in the table is the integral $-(8/(2t))\int_0^t dt'\int_0^{t'}dt''$ over an integrand that is the product of the entries in the first two columns and entries in the first two rows of the table. Only one half of the table is presented here, the other half is obtained by exchanging ω_{rf1} and ω_{rf2}, and ϕ_1 and ϕ_2.

		$\cos(\omega_{\text{rf1}}t''+\phi_1)$		
		$\cos\omega_0 t''$	$\sin\omega_0 t''$	1
$\cos(\omega_{\text{rf1}}t'+\phi_1)$	$\cos\omega_0 t'$	0	$\frac{\omega_0}{\omega_0^2-\omega_{\text{rf1}}^2}$	0
	$\sin\omega_0 t'$	$\frac{-\omega_0}{\omega_0^2-\omega_{\text{rf1}}^2}$	0	0
	1	0	0	0
$\cos(\omega_{\text{rf2}}t'+\phi_2)$	$\cos\omega_0 t'$	0	0	$\frac{-\sin(\phi_1+\phi_2)}{\omega_{\text{rf1}}}$
	$\sin\omega_0 t'$	0	0	$\frac{-\cos(\phi_1+\phi_2)}{\omega_{\text{rf1}}}$
	1	$\frac{\sin(\phi_1+\phi_2)}{\omega_{\text{rf2}}}$	$\frac{\cos(\phi_1+\phi_2)}{\omega_{\text{rf2}}}$	0

It is straightforward to extend the above argument to two-photon excitation with two rf fields whose frequencies sum to the resonant frequency ($\omega_{\text{rf1}}+\omega_{\text{rf2}}=\omega_n$). Cross terms inside the integral of Eq. (6) of the form $e^{i\omega_n t'}\cos\omega_{\text{rf1}}t'\cos\omega_{\text{rf2}}t''$ that do not vanish after integration lead to two-photon, two-color excitation. Higher order terms of the Magnus expansion will lead in a similar fashion to three and greater photon excitation.

B. Explicit calculation for two-color excitation in NMR

We consider an isolated spin in an external magnetic field of strength $B_0=\omega_0/\gamma$ in the presence of two colinear rf fields, as would be the case in a doubly tuned rf coil, applied at an angle α to the external field. We define the z axis to lie along the static field and choose the x axis so that the rf fields lie in the x-z plane. With the two rf fields having respective strengths B_1 and B_2, phases ϕ_1 and ϕ_2, and frequencies $\omega_{\text{rf1}}=(\omega_0-\delta)/2$ and $\omega_{\text{rf2}}=(\omega_0+\delta)/2$, so that $\omega_{\text{rf1}}+\omega_{\text{rf2}}=\omega_0$, the Hamiltonian may be written as

$$\begin{aligned}\hat{\mathcal{H}}(t)=&\omega_0 I_z+\gamma B_1(I_x\sin\alpha+I_z\cos\alpha)\cos(\omega_{\text{rf1}}t+\phi_1)\\&+\gamma B_2(I_x\sin\alpha+I_z\cos\alpha)\cos(\omega_{\text{rf2}}t+\phi_2).\end{aligned} \tag{7}$$

Transforming into an interaction frame with $\hat{U}=e^{i\omega_0 tI_z}$, the effective Hamiltonian becomes

$$\begin{aligned}\hat{\mathcal{H}}_{\text{eff}}(t)=&\gamma B_1[(I_x\cos\omega_0 t+I_y\sin\omega_0 t)\sin\alpha\\&+I_z\cos\alpha]\cos(\omega_{\text{rf1}}t+\phi_1)+\gamma B_2[(I_x\cos\omega_0 t\\&+I_y\sin\omega_0 t)\sin\alpha+I_z\cos\alpha]\cos(\omega_{\text{rf2}}t+\phi_2).\end{aligned} \tag{8}$$

Using the commutation relations of spin operators and the double integrals over trigonometric functions summarized in Table I, the two-color excitation Hamiltonian may be calculated from Eq. (6) yielding

$$\hat{\mathcal{H}}_{\text{eff}}^{(1)} = \omega_{\text{nut}}[I_x \cos(\phi_1+\phi_2) - I_y \sin(\phi_1+\phi_2)] + (\Delta\omega_1^{\text{BS}} + \Delta\omega_2^{\text{BS}})I_z, \tag{9}$$

where

$$\omega_{\text{nut}} = \frac{(\frac{1}{2}\gamma B_2 \sin\alpha)(\frac{1}{2}\gamma B_1 \cos\alpha)}{\omega_{\text{rf1}}} + \frac{(\frac{1}{2}\gamma B_1 \sin\alpha)(\frac{1}{2}\gamma B_2 \cos\alpha)}{\omega_{\text{rf2}}} = \frac{\gamma B_1 B_2 \sin 2\alpha}{2B_0\left[1-\left(\frac{\delta}{\omega_0}\right)^2\right]} \tag{10}$$

and

$$\Delta\omega_i^{\text{BS}} = \frac{-\gamma B_i^2 \sin^2\alpha}{4B_0\left[1-\left(\frac{\omega_{\text{rf}i}}{\omega_0}\right)^2\right]}. \tag{11}$$

The first term in Eq. (9) results in nutation at an angular frequency ω_{nut}, while the second is responsible for a frequency shift, known as the Bloch-Siegert (BS) shift,[6] and is the sum of two shifts, one due to each of the rf fields. As a consequence of the presence of both B_1 and B_2 in Eq. (10), the nutation occurs only if both rf fields are present, while each of the shifts of Eq. (11) persists if only its respective rf field is applied. The α dependence of Eq. (10) reveals that two-photon excitation occurs only if the coil has components both parallel and perpendicular to B_0. This requirement reflects the fact that two-photon transitions between levels with $|\Delta m| = 1$ require one transverse (σ^+ or σ^-) and one longitudinal π photon in order to conserve angular momentum.[20] The first equality of Eq. (10) is written to emphasize that the nutation predicted arises as the result of two separate processes, the first corresponding to a π-photon absorbed at ω_{rf1} and a σ-photon absorbed at ω_{rf2} while the second corresponds to a π-photon at ω_{rf2} and a σ-photon at ω_{rf1}. For an experimental setup in which one rf field is applied along z, while the other is applied along x, only one term would be present.

In what follows, we take ω_0 to be the receiver reference frequency. In the presence of a resonance offset, where ω_0 is not exactly the nuclear resonance frequency, the offset adds in a straightforward fashion to the BS shifts of Eq. (9).

Equation (10) reveals that the nutation frequency increases as δ, the difference between the two excitation frequencies, increases, as is depicted in Fig. 1. In fact the nutation rate appears to diverge at $\delta = \omega_0$. Our AHT treatment breaks down when terms in the integrand of Eq. (6) vary slowly compared to the spin evolution time. This is certainly the case in the vicinity of $\delta = \omega_0$, and in fact near $\delta/\omega_0 = m$ for any integer m. The region of δ around $m\omega_0$ in which Eq. (9) cannot be applied is given roughly by the larger of the rf amplitudes multiplied by γ. Except for the cases of $m = 1$ and 3 where on-resonance excitation (by ω_{rf1} and ω_{rf2}, respectively) dominates, our approach is again valid exactly at $\delta/\omega_0 = m$, but the results of the integration of Eq. (6) in Table I no longer apply, and the integrals must be reevaluated for these special cases.

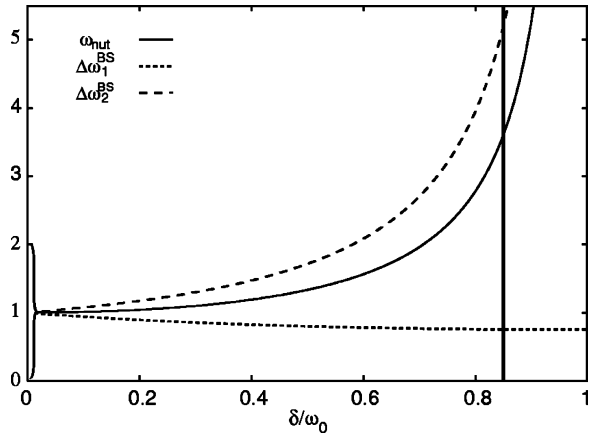

FIG. 1. Relative two-photon nutation rate (solid curve) and BS shifts (dashed curves) as functions of the choice of rf frequencies, based on Eqs. (10) and (11). Near $\delta = 0$, additional terms become important and the relative phase of the two rf fields dictates whether excitation is constructive or destructive. The vertical line at 0.85 represents our choice of irradiation frequencies for excitation of protons.

If both rf fields are applied at $\omega_0/2$ ($\delta = 0$), the cross terms surviving integration are displayed in Table II, yielding

$$\hat{\mathcal{H}}_{\text{eff}}^{(1)} = \frac{\gamma \sin 2\alpha}{4B_0}\{[B_1^2 \cos 2\phi_1 + B_2^2 \cos 2\phi_2 + 2B_1B_2 \cos(\phi_1+\phi_2)]I_x - [B_1^2 \sin 2\phi_1 + B_2^2 \sin 2\phi_2 + 2B_1B_2 \sin(\phi_1+\phi_2)]I_y\} - \frac{\gamma \sin^2\alpha}{3B_0}[B_1^2 + B_2^2 + 2B_1B_2 \cos(\phi_1-\phi_2)]I_z. \tag{12}$$

Depending on the relative phases and strengths of the two rf fields, the nutation rate varies between 0 and twice that given by Eq. (10). In practice, for irradiation at $\omega_0/2$, typically only one rf field is applied, reducing the nutation rate by a factor of 4. In this case we recover the previously derived result[5] for two-photon excitation:

$$\hat{\mathcal{H}}_{\text{eff}}^{(1)} = \frac{\gamma B_1^2 \sin 2\alpha}{4B_0}(I_x \cos 2\phi - I_y \sin 2\phi) - \frac{\gamma B_1^2 \sin^2\alpha}{3B_0} I_z. \tag{13}$$

For $\delta > \omega_0$, ω_{rf2} becomes negative, and resonance cor-

TABLE II. Integrals $-(8/(2t))\int_0^t dt' \int_0^{t'} dt''$ for $\delta = 0$, i.e., $\omega_{\text{rf1}} = \omega_{\text{rf2}} = \omega_0/2 = \omega_{\text{rf}}$, interpreted in a similar fashion to Table I.

		$\cos(\omega_{\text{rf}}t''+\phi_2)$		
		$\cos\omega_0 t''$	$\sin\omega_0 t''$	1
$\cos(\omega_{\text{rf}}t'+\phi_1)$	$\cos\omega_0 t'$	$-\frac{2\sin(\phi_1-\phi_2)}{3\omega_0}$	$\frac{4\cos(\phi_1-\phi_2)}{3\omega_0}$	$-\frac{2\sin(\phi_1+\phi_2)}{\omega_0}$
	$\sin\omega_0 t'$	$-\frac{4\cos(\phi_1-\phi_2)}{3\omega_0}$	$-\frac{2\sin(\phi_1-\phi_2)}{3\omega_0}$	$-\frac{2\cos(\phi_1+\phi_2)}{\omega_0}$
	1	$\frac{2\sin(\phi_1+\phi_2)}{\omega_0}$	$\frac{2\cos(\phi_1+\phi_2)}{\omega_0}$	$\frac{4\sin(\phi_1-\phi_2)}{\omega_0}$

responds to the difference frequency, $\omega_{rf1}-|\omega_{rf2}|$. For $1<\delta/\omega_0<3$, one of the excitation frequencies is above resonance and the other below. For the special condition $\delta/\omega_0=2$ ($\omega_{rf1}=-\omega_0/2$ and $\omega_{rf2}=3\omega_0/2$) both two-color and half-frequency excitation will occur. Our present approach remains valid, but requires a recalculation of the integrals in Table I. Beyond $\delta/\omega_0>3$, the absolute values of both excitation frequencies are above resonance.

III. EXPERIMENTAL SETUP

Two-color excited ^{1}H spectra were acquired from a sample of H_2O in a sealed 4 mm magic-angle-spinning (MAS) rotor. Spectra were obtained on a Varian ^{UNITY}INOVA 400 spectrometer with a Varian Chemagnetics HFX MAS probe tuned to 30, 370, and 400 MHz. This MAS probe was chosen not only for its triple-resonance tuning, but also for the oblique angle the rf coil makes with the external field, providing $\alpha=54.7°$. Spectra were acquired, without MAS, on the 400 MHz channel with irradiation on the 30 and 370 MHz channels. The lower excitation frequency, $\omega_{rf1}/2\pi$ was fixed at 30.00 MHz, while the exact value of $\omega_{rf2}/2\pi$ (369.74 MHz) was set to the difference between the desired receiver reference (399.74 MHz) and $\omega_{rf1}/2\pi$. A 400 MHz selective bandpass filter was used on the detection channel to minimize 30 and 370 MHz rf feedthrough to the receiver.

All spectra were obtained with excitation powers of 600 and 300 W on the 30 and 370 MHz channels, respectively, unless otherwise noted. Each spectrum was obtained with a single scan, although phase coherence between transmitter and receiver channels did allow for signal averaging.

Calibrations of the off-resonance field strengths were performed on ^{14}N and ^{19}F using acetonitrile and poly(tetrafluoroethylene) samples with the probe retuned to 28.88 and 376.08 MHz.

Adiabatic passage was performed with a rf frequency sweep on the 30 MHz channel, implemented as an accelerating phase shift to obtain an 8 kHz sweep width centered about the proton resonance line. Phase steps were taken every 20 μs during the 50 ms detection time with acquisition of a complex point every 20 μs.

IV. RESULTS

Figure 2(a) shows the time-domain signal acquired during nutation due to two-color excitation. The trace begins when the receiver and one of the rf channels are turned on. Nutation begins and a nonzero signal is observed when the second rf channel is turned on 120 μs later. An identical plot is obtained if the order in which the rf channels are turned on is reversed.

To obtain an accurate measure of ω_{nut}, the rf frequencies were selected to sum to the ordinary resonance frequency plus the BS shift ($\omega_{rf1}+\omega_{rf2}=\omega_0+\Delta\omega_1^{BS}+\Delta\omega_1^{BS}$) so that only the I_x term in Eq. (9) is responsible for the observed nutation.

The contributions to the BS shift of the two rf fields may be measured by allowing the magnetization to evolve with no rf fields present [Fig. 2(b)], with only the 370 MHz rf present [Fig. 2(c)], or with only the 30 MHz rf present [Fig. 2(d)]. We find shifts of $\Delta\omega_1^{BS}/2\pi=1220$ Hz and $\Delta\omega_2^{BS}/2\pi=150$ Hz for the 30 and 370 MHz channels, respectively. From these values, using Eq. (11), we calculate respective rf field strengths of $\gamma B_1/2\pi=1710$ kHz and $\gamma B_2/2\pi=228$ kHz (expressed in units of proton frequency), and, using Eq. (10), a nutation frequency of 1.65 kHz which agrees well with the 1.71 kHz that may be measured directly from Fig. 2(a).

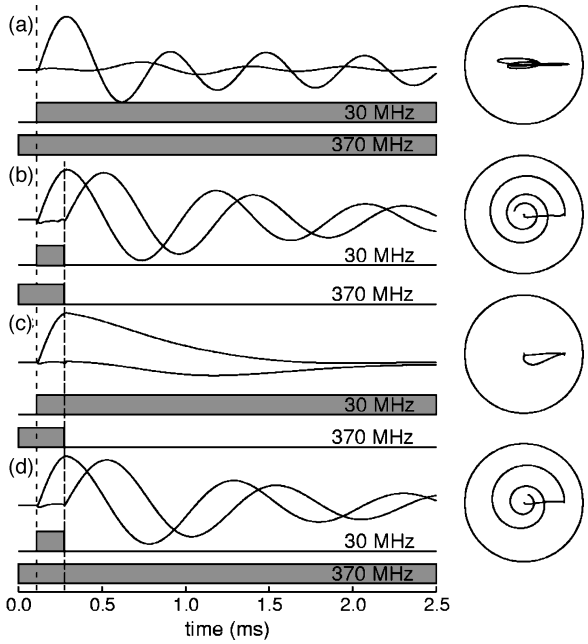

FIG. 2. Two-color excitation of ^{1}H spins in H_2O. (a) Direct observation of nutation. The transmitter frequencies were chosen to be exactly on resonance, including the BS shifts, during irradiation. (b) Excitation followed by free precession. (c) and (d) Excitation followed by precession with continued irradiation at 30 MHz (c) or 370 MHz (d). The gray bars indicate the times during which the rf channels were turned on. The panels on the right are projections of the signals in the complex plane. The precession frequencies displayed following excitation in (b), (c), and (d) are due to the BS shift terms of Eq. (11).

The rf field strengths calculated from the BS shifts also compare well with the directly measured values of 1630 kHz and 190 kHz obtained from calibrations on ^{14}N and ^{19}F. The expected nutation frequency from the calibrations is 1.33 kHz. The differences between these and the directly measured values can be attributed to differences in probe and amplifier performance at the different frequencies used for the experiments and calibrations.

Potential mixing of the 30 MHz and 370 MHz rf's by nonlinearities in passive probe components was investigated by coupling the probe's 400 MHz channel directly into an oscilloscope during continuous irradiation on both the 30 and 370 MHz channels. No detectable 400 MHz rf was observed, whereas the level of on-resonance rf excitation required to achieve a comparable nutation frequency was more than three orders of magnitude (in voltage) greater than the detection limit using the oscilloscope. This result, in concert with the fact that we were able to detect a NMR signal during excitation without a dc offset as would be expected from any

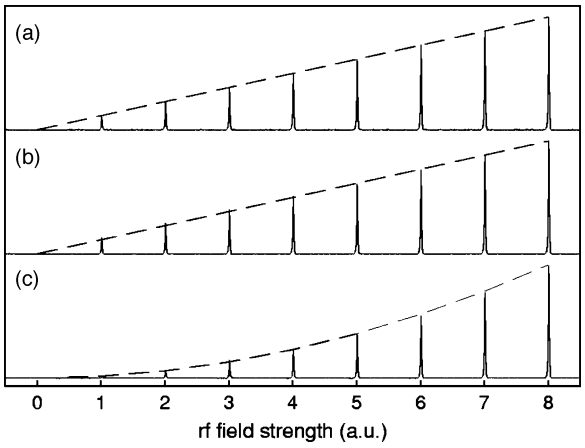

FIG. 3. ^{1}H spectra of H_2O obtained following two-color excitation with a fixed length (10 μs) pulse and an increasing rf field strength on (a) the 370 MHz channel, (b) the 30 MHz channel, and (c) both channels simultaneously. The strongest pulses correspond to a tip angle of 0.3°. The dashed lines are linear (a) and (b) or quadratic (c) guides to the eye.

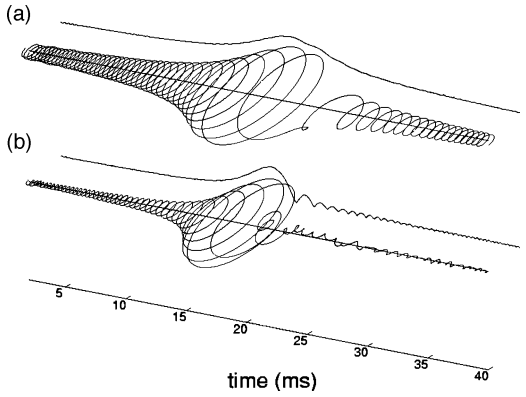

FIG. 4. Observation of frequency sweeps through resonance. The data, depicted here in a frame rotating at a constant 400 MHz, are plotted to show the transverse magnetization in a plane perpendicular to the time axis. The magnitude of the transverse magnetization is shown above each data set. In (a), the excitation powers were 600 and 300 W on the 30 and 370 MHz channels while in (b) the power at 30 MHz was reduced to 10 W.

rf mixing, leads us to believe that the signal we observe is due entirely to two-photon excitation.

Figure 3 depicts a series of two-photon-excited water spectra that display a linear increase in amplitude with increasing rf field strength for each channel separately [Figs. 3(a) and 3(b)] as expected from Eq. (9). When the rf field strengths are ramped simultaneously, the amplitude of the observed signal increases quadratically [Fig. 3(c)]. These data highlight the feature of two-color excitation that the amplitude, frequency, and phase of the effective field all vary linearly with their counterparts on each of the applied rf fields. Thus full control over the effective field may be obtained without any amplitude, phase, or frequency modulation of one of the transmitters.

The evolution of the nuclear magnetization during an adiabatic fast passage is displayed in Fig. 4(a). One rf channel remains purely sinusoidal while the other is swept through the two-color resonance condition. Typically, adiabatic fast passage experiments are visualized in a frame rotating with the excitation field in which case magnetization follows the effective field from the positive to negative z axis in the x-z plane.[21] Here, we detect in a frame rotating at constant frequency (on-resonance) so that we observe a signal whose frequency decreases as resonance is approached, becoming zero on resonance and changing sign after resonance is passed. Due to the BS shift, the center of the observed peak does not fall in the center of the sweep and we observe the peak move towards the center as the rf power is decreased. In Fig. 4(b), by reducing the rf field strength, we have entered the linear fast passage regime[21] in which some of the magnetization is left in the transverse plane resulting in an asymmetric peak consisting of the swept peak plus a transient decay. By stopping midway through an adiabatic fast passage, or by optimizing the effective field strength and sweep rate for a linear fast passage (known as a chirped pulse[22]), one can, in principle, achieve $\pi/2$ pulses with very small rf field strengths.

V. DISCUSSION

A. Advantages and disadvantages of two-color excitation

While retaining the features resulting from the separation of excitation and detection frequencies that were introduced with half-frequency excitation, two-color excitation offers several further advantages. The most prominent of these is an improved excitation strength that increases as the difference between the two rf frequencies increases (Fig. 1). At the frequencies used here ($\delta/\omega_0 = 0.85$), Eq. (10) gives a 3.5-fold improvement in nutation frequency compared to excitation at $\omega_0/2$ assuming the same total power applied to the probe, neglecting variations in probe performance as a function of frequency. Further substantial improvements are possible with a modest increase in δ. Along with the limits to the validity of Eq. (9) set by the proximity of δ to $m\omega_0$ compared to the rf amplitudes discussed above, the practical difficulties associated with applying rf close to resonance while maintaining acceptable isolation between transmission and reception channels may ultimately limit the range of accessible δ.

A second advantage of two-color excitation over excitation at $\omega_0/2$ is the fact that the fidelity requirements of the rf fields are greatly reduced. Harmonic output of rf power amplifiers will not generally contribute to any excitation nor interfere with detection, except for unfortunate choices of δ (for example, where $\delta/\omega_0 = 2/3$ so that $\omega_{rf1} = \omega_0/3$) that are easily avoided. This greatly relaxes the need for high power rf band-pass filters on the excitation channels. Provided that any nonlinearities in the electrical response of probe components are symmetric with respect to the sign of the voltage, such nonlinearities will not mix the two excitation frequencies to produce ω_0 in the absence of a dc offset.

The two-color technique can be performed on most commercial spectrometers with no special hardware or software modification aside from retuning of a MAS probe. It does, however, require three rf synthesizers operating from the same reference clock.

Two-color excitation suffers from the disadvantage of

requiring a triply tuned probe in order to observe signals from a single nuclear species. Our implementation also employed two rf transmitters and power amplifiers; however, it may be possible in some cases to amplify the two rf excitation signals in the same power amplifier and couple them to the probe on a single port.

B. Optimizations

In order to achieve the maximum ω_{nut} possible, it is clear from Eq. (10) that B_1 and B_2 should be as large as possible, and δ should be as close to ω_0 as possible. The restriction that the rf amplitudes remain small compared to $|\delta-\omega_0|$ (as δ approaches ω_0) for Eq. (9) to apply, implies a trade-off: as B_1 and B_2 are increased, the required separation between δ and ω_0 increases, attenuating the boost to ω_{nut} provided by the denominator of Eq. (10). At some point as B_1 and B_2 are increased, the limits they place on δ actually cause a decrease in ω_{nut}. This limit is not reached, however, until the rf fields are a sizable fraction of B_0.

A more likely limitation on the field strengths may be placed by the probe's power handling capability, and we consider the optimal distribution of the total rf power (P_T) between the two rf channels. The rf field produced in an NMR coil by an rf pulse having power P_1 is $B_1=k\sqrt{P_1/R(\omega_{\mathrm{rf1}})}$ where k is a constant of proportionality fixed for a given probe and $R(\omega)$ is the resistance of the coil, generally a complicated function of frequency.[23] Substituting this relation into Eq. (10) we find

$$\omega_{\mathrm{nut}}\propto kP_T\left[\frac{r_1(1-r_1)}{R(\omega_{\mathrm{rf1}})R(\omega_{\mathrm{rf2}})}\right]^{1/2}, \tag{14}$$

where $P_T=P_1+P_2$ is the total rf power and $r_1=P_1/P_T$ is the fraction applied at ω_{rf1}. The optimal choice of r_1 is clearly given by 1/2, independent of the choice of frequencies and the functional form of $R(\omega)$, and corresponds to equal power applied to the two channels. In our experiments with a value of $r_1=0.67$, we achieved 94% of the optimal efficiency, based on limiting the input power to the probe at 900 W.

C. Opportunities for nonlinear processes in NMR

Despite the increase in ω_{nut} afforded by two-color excitation over half-frequency excitation, the nutation frequencies produced remain small compared to those required for many potential applications. Ongoing developments in the use of microcoils, with which significantly stronger rf fields may be produced,[24–27] may provide opportunities for practical applications for two-photon excitation and other nonlinear effects in NMR.

Any case where minimizing the receiver deadtime is important would be a clear candidate for two-photon excitation. An example is wide-line NMR, especially in the presence of molecular motion, where echo techniques to refocus rapidly decaying NMR signals are ineffective. Clearly, for broadband excitation, an adequate effective field strength is a key requirement.

The potentially important application of simultaneous homonuclear decoupling and detection[5] that is currently being pursued using microcoil probes elsewhere[24] may also benefit from the boost in nutation frequency provided by two-color excitation.

Two-color excitation also offers the opportunity for more exotic, though potentially less practical manipulation and detection of spin systems. The excitation condition, $\omega_{\mathrm{rf1}}+\omega_{\mathrm{rf2}}=\omega_0$, leaves one degree of freedom and allows the selection of one of the frequencies to correspond to another nuclear resonance frequency, enabling the simultaneous excitation of two nuclear species with a triply tuned probe. This may be useful, for example, to decouple one nucleus while simultaneously exciting another with a two-photon process. In a similar arrangement, with careful adjustment of rf amplitudes, one could achieve a Hartmann-Hahn match between two nuclear species with one species spin-locked directly (at ω_{rf1} or ω_{rf2}) while the other is spin-locked with a two-photon field (at $\omega_{\mathrm{rf1}}+\omega_{\mathrm{rf2}}$).

A final proposal is motivated by a close inspection of the nutation signal in Fig. 2(a), which reveals a decay that cannot be described by a single exponential but rather has a quickly and slowly decaying component. We attribute the quickly decaying component to inhomogeneity of the rf fields, with the slowly decaying part due to a region of high homogeneity in the center of the coil. Rf inhomogeneity is magnified compared to on-resonance excitation due ω_{nut}'s quadratic dependence on field strength. In principle, if the field inhomogeneity was known or deliberately nonuniform, the BS shift, under irradiation with one or more off-resonance rf fields, could be used for spatial localization without the use of a separate gradient coil. Such an implementation may have a niche for certain microimaging applications.

VI. CONCLUSIONS

We have shown that two-photon excitation is a consequence of first-order terms in the Magnus expansion and occurs whenever two applied rf frequencies sum to or differ by ω_0. Excitation away from half the transition frequency, referred to as two-color excitation, presents significant improvements in the excitation strength as well as other practical benefits. We have demonstrated that two-color excitation is robust and amenable to current NMR spectrometer hardware and software with minimal modification. Ongoing developments of microcoil probe technology may provide opportunities for a variety of practical applications based on two-photon excitation and other nonlinear effects.

ACKNOWLEDGMENTS

This work was supported by a grant from the Natural Sciences and Engineering Research Council (NSERC) of Canada. The Varian NMR spectrometer was purchased with the assistance of the Canada Foundation for Innovation and the BC Knowledge Development Fund. P.E. thanks NSERC for a postgraduate scholarship.

[1] R. R. Ernst, *Principles of Nuclear Magnetic Resonance in One and Two Dimensions* (Oxford University Press, Oxford, 1987).
[2] S. Meiboom and D. Gill, Rev. Sci. Instrum. **29**, 688 (1958).
[3] J. S. Waugh, L. M. Huber, and U. Haeberlen, Phys. Rev. Lett. **20**, 180 (1968).
[4] E. Fukushima and S. B. W. Roeder, *Experimental Pulse NMR: A Nuts and Bolts Approach*, (Westview, Boulder, Colorado, 1981) Chap. 4.
[5] C. A. Michal, J. Chem. Phys. **118**, 3451 (2003).
[6] F. Bloch and A. Siegert, Phys. Rev. **57**, 522 (1940).
[7] J. Margerie and J. Brossel, C. R. Acad. Sci. (Paris) **241**, 373 (1955).
[8] J. Winter, C. R. Acad. Sci. (Paris) **241**, 375 (1955).
[9] W. Anderson, Phys. Rev. **104**, 850 (1956).
[10] W. A. Anderson, Phys. Rev. **102**, 151 (1956).
[11] Y. Zur, M. H. Levitt, and S. Vega, J. Chem. Phys. **78**, 5293 (1983).
[12] A. Abragam, *Principles of Nuclear Magnetism*, (Oxford University Press, Oxford, 1961), Chap. 2.
[13] J. H. Shirley, Phys. Rev. **138**, B979 (1965).
[14] G. Bodenhausen, Prog. Nucl. Magn. Reson. Spectrosc. **14**, 137 (1981).
[15] P. T. Eles and C. A. Michal, Chem. Phys. Lett. **376**, 268 (2003).
[16] R. R. Ernst, J. Magn. Reson. **3**, 10 (1970).
[17] R. Kaiser, J. Magn. Reson. **3**, 28 (1970).
[18] U. Haeberlen and J. S. Waugh, Phys. Rev. **175**, 453 (1968).
[19] W. Magnus, Commun. Pure Appl. Math. **7**, 649 (1954).
[20] C. Cohen-Tannoudji, B. Diu, and F. Lalo, *Quantum Mechanics* (Wiley, New York, 1977).
[21] R. R. Ernst, Adv. Magn. Reson. **2**, 72 (1966).
[22] J.-M. Böhlen and G. Bodenhausen, J. Magn. Reson., Ser. A **102**, 293 (1993).
[23] D. I. Hoult and R. E. Richards, J. Magn. Reson. **24**, 71 (1976).
[24] K. Yamauchi, J. W. G. Janssen, and A. P. M. Kentgens, J. Magn. Reson. **167**, 87 (2003).
[25] A. G. Webb and S. C. Grant, J. Magn. Reson. **113**, 83 (1996).
[26] T. L. Peck, R. L. Magin, and P. C. Lauterbur, J. Magn. Reson., Ser. B **108**, 114 (1995).
[27] A. G. Webb, Prog. Nucl. Magn. Reson. Spectrosc. **31**, 1 (1997).